Chapter 5

Experimental Setup

5.1 Microwave Bridge

The microwave bridge setup of the spectrometer existed in two different configurations. Since the first configuration did not allow for phase sensitive detection, it was upgraded in a second step to phase coherence between transmitter (source) and receiver (detector). Since most of the measurements were performed with the first setup, this will be described more in detail. The differences to the final one will then be highlighted in the following section.

5.1.1 Transmitter

The microwave source (Farran Technology Ltd. 1997) is a frequency–tripled phase–locked 120 GHz Gunn Oscillator.

Since free–running Gunn diodes have linewidths in the MHz range, they cannot be used as spectroscopic sources as such, but have to be phase–locked to a more stable oscillator. In our case, phase–lock is established with respect to an internal dielectric resonator oscillator (DRO) as depicted in Figure 5.1 A small part of the output power of the 120 GHz Gunn oscillator with frequency f_S is coupled into a harmonic mixer via a directional coupler. The

local oscillator (LO) input of this mixer is fed by a highly stable DRO running at 19.9833 GHz. The intermediate frequency (IF) then is the difference between the 120 GHz input signal (RF) and the 6th harmonic of the LO:

$$f_{IF} = f_S - N f_\mu \tag{5.1}$$

where $N = 6$, so $f_{IF} = 100\text{MHz} + \Delta f_S$ where Δf_S is the frequency offset (error signal) of the 120 GHz Gunn oscillator. f_{IF} is then passed through the LO port and a triplexer to a phase lock unit (XL microwave Model 800A). This unit supplies a bias voltage to the Gunn Oscillator plus a correction voltage which is proportional to the difference between f_{IF} and a reference frequency supplied by a highly stabilized 100 MHz reference source.

The main power output of the Gunn source is finally fed into a tripler, providing a specified output power of ≈ 0.9 mW at 360 GHz and a line width < 2 kHz FWHM (full width at half maximum). The frequency stability is specified to $\pm$ 30 ppm (parts per million).

The overall transmitter phase noise at 360 GHz resulting from this setup depends on the stability of the reference DRO and the bandwidth of the phase–lock loop (PLL). The phase reference in this case is the DRO source.

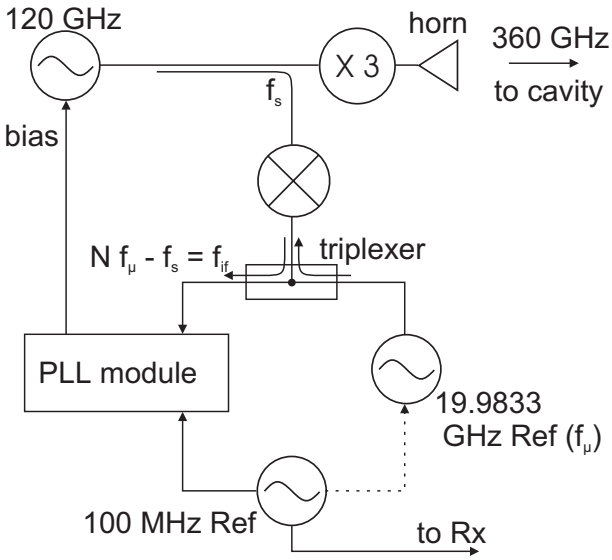

Figure 5.1: Phase locking scheme of transmitter system

5.1.2 Receiver

For detection a heterodyne mixer scheme is employed. In contrast to a homodyne detection setup, in a heterodyne system the signal is not directly converted to a DC signal, but downconverted to an intermediate frequency in the order of some GHz. This is to avoid the noise figure of the system to be governed by the so–called $1/f$–noise. For the final downconversion of the IF frequency one can then employ low–noise components that are readily available at these frequencies.

The central component of the receiver (Farran Technology Ltd. 1997) is a subharmonic mixer detector with a detection bandwidth of 100 MHz (Figure 5.2). In contrast to a fundamental mixer, in a subharmonic mixer the RF signal is mixed not with the fundamental frequency of the LO input but with a higher harmonic. The local oscillator can therefore operate at a lower frequency with all the advantages of lower frequency components. The disadvantage of course is the less efficient mixing process.

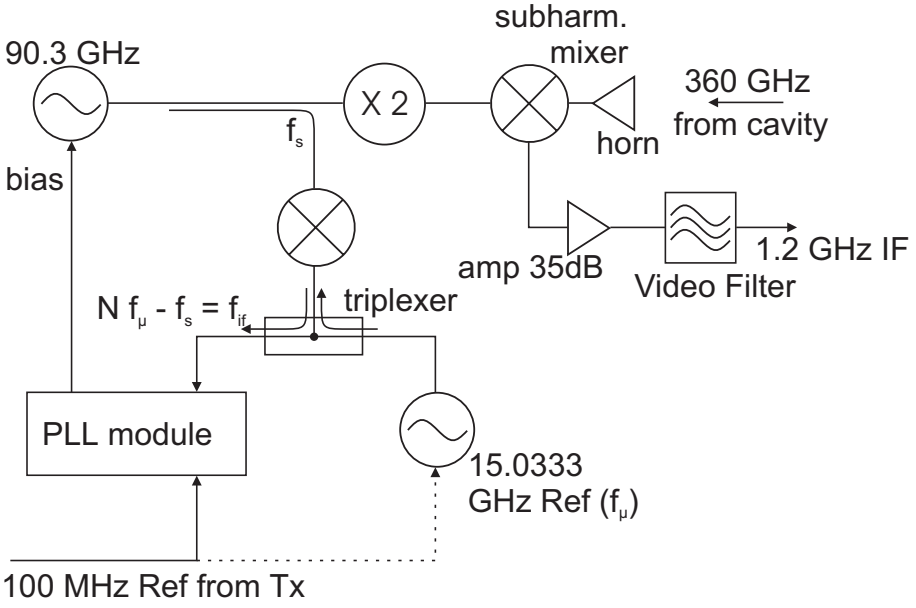

Figure 5.2: Phase locking scheme of receiver system

The LO is provided by a phase–locked, doubled 90.3 GHz Gunn oscillator. The PLL setup is completely analogous to the transmitter module. The necessary RF reference is supplied directly from the 100 MHz source of the transmitter control module. The microwave reference DRO source provides a frequency of $f_\mu = 15.0333$ GHz. The stabilized output is then frequency doubled to yield a LO frequency of 180.6 GHz.

With the subharmonic mixer running at the 2nd LO harmonic, the EPR signal at 360 GHz is downconverted with a LO frequency of 361.2 GHz, so the resulting IF frequency is 1.2 GHz. This is then passed through a low noise amplifier with a 35 dB gain and a video filter.

The noise figure of the complete receiver module is 12 dB double side band noise (DSB – this corresponds to half the single side band noise – SSB – of 15 dB). This performance is comparable to the most sensitive bolometer detectors available.

Since the detection bandwidth is 100 MHz, however, with this setup the detection of transients on a time scale down to 10 ns can be achieved (compared to 1 μs for commercially available InSb hot electron bolometers). This is of central importance for the planned upgrade of the spectrometer to a time–resolved EPR setup with high time resolution.

Analogous to the transmitter PLL scheme, the phase reference for the local Oscillator is provided by the microwave reference DRO. This means that transmitter and receiver are both phase stabilized, but not with respect to each other. For phase coherence between transmitter and receiver to be established, the respective DRO sources also have to be locked to a common master reference frequency (indicated by the dashed lines in figure 5.1 and figure 5.2).

The first setup therefore did not yet allow for phase sensitive detection. As a result the final downconversion to DC was performed as a magnitude detection only; in this case we used a spectrum analyzer (Hewlett & Packard

HP 8555 A / 8552 B). Its output was fed to a lock–in detector (Stanford Research SR830), which in turn was interfaced to a Personal Computer.

5.1.3 Phase–Coherent Bridge

To be phase–locked to the master reference frequency, the intermediate lock frequency sources (f_μ) need to operate at a direct multiple of this frequency. This was not the case for the first microwave bridge configuration, whith the DRO outputs not being direct multiples of 100 MHz, so a different master frequency had to be chosen. This of course immediately required a retuning of all other frequencies as well.

To establish phase coherence between transmitter and receiver, the system was modified to employ a different set of reference frequencies. The new frequencies are as follows:

- Transmitter: Gunn oscillator $f_S = 120.01$ GHz
  RF Master reference $f_{RF} = 10$ MHz
  microwave reference DRO $f_\mu = 20.000$ GHz
  final transmitter output frequency $f_{Tx} = 360.03$ GHz

- Receiver: Gunn oscillator $f_S = 90.31$ GHz
  microwave reference DRO $f_\mu = 15.050$ GHz
  final IF frequency 1.21 GHz

At the current stage of development, the new frequencies have been established, but the sources still operate independently of each other. Once they are locked, in the upgraded system the down conversion will eventually be achieved with a Quadrature IF mixer (Anaren Microwave Ltd. 1998). The LO for this mixer is provided by a 1.21 GHz dielectric resonator oscillator (DRO) which again is phase–locked to the 10 MHz master oscillator (see figure 5.3). Since in a quadrature mixer both in–phase and out–of–phase signal

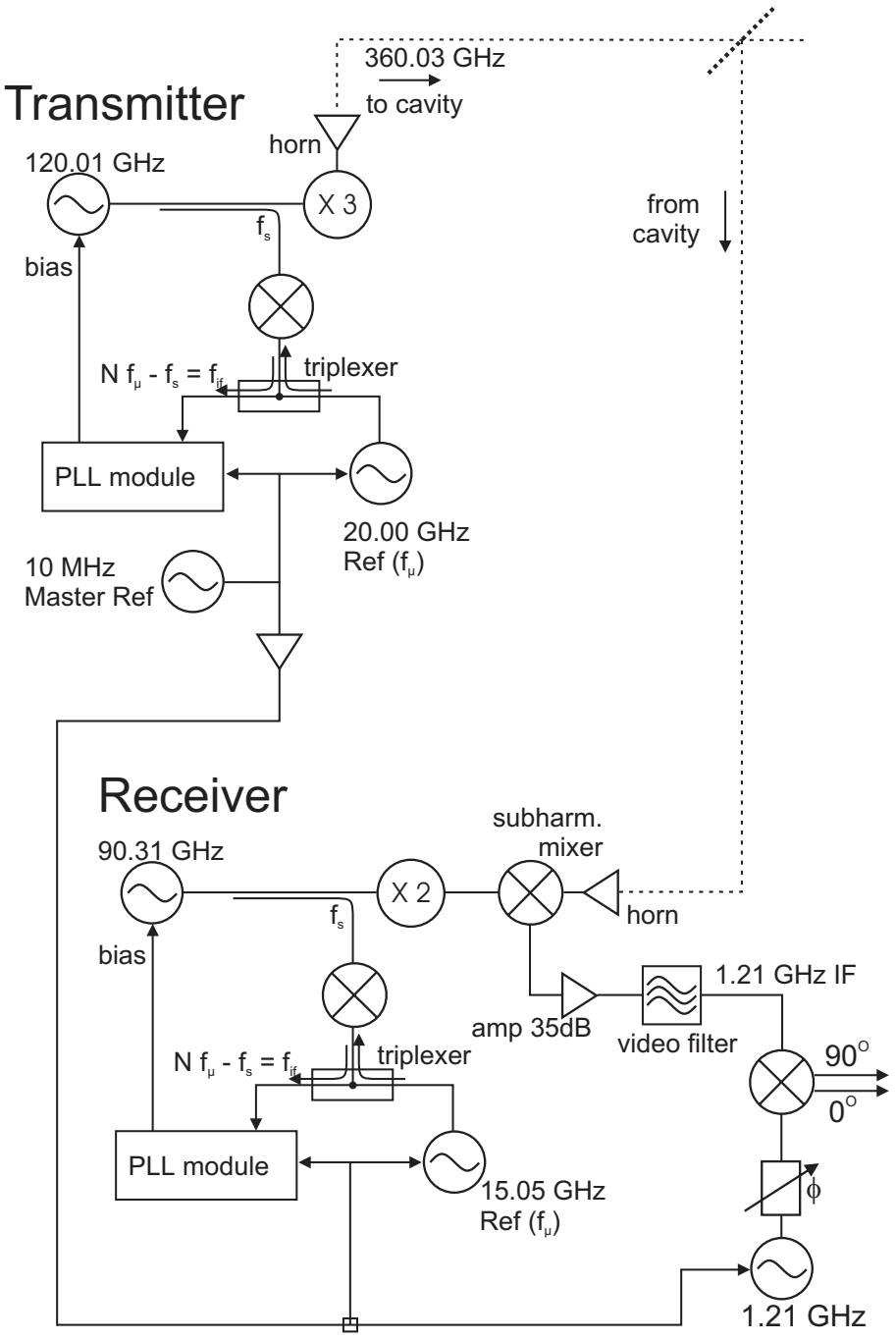

Figure 5.3: Final phase lock scheme of complete MW system with 10 MHz master reference frequency and phase sensitive downconversion stage.

components are generated simultaneously, both the absorptive and dispersive signal components can be detected in a single experimental run.

It should be noted, that in principle the problems that arise from phase locking two high–frequency sources to each other, could be avoided by using a setup with a reference arm, which supplies a phase coherent LO frequency. This however requires higher microwave power levels since the power for the reference arm must be diverged from the excitation channel. This obviously is not feasible in our case. Furthermore, one then has to resort to a homodyne detection scheme.

5.2 Quasi–Optical Transmission Line

5.2.1 Components and Techniques

At wavelengths in the mm– and sub–mm–range fundamental mode waveguides become exceedingly lossy (J. C. G. LeSurf 1990, Käs & Pauli 1991). While at frequencies of 95 and even 150 GHz fundamental mode waveguides have successfully been employed (Burghaus et al. 1992, Grinberg et al. 1983), even there, for longer sections oversized waveguides were used.

In our spectrometer (see Figure 5.4) we therefore employ a quasi–optical transmission line setup (Farran Technology Ltd. 1997) in which a Gaussian beam is launched via a corrugated horn antenna into free space. Where free space propagation is not feasible, corrugated oversized waveguides have been used (see below).

In perfect analogy to geometric optics, to refocus a diverging beam one can employ either curved mirrors or lenses. In contrast to mirrors, lenses do not directly obstruct the beam path, and therefore allow for a more straightforward design since unnecessary folding of the beam path can be avoided. However, they can be the origin of standing waves in the system and cause dielectric losses.

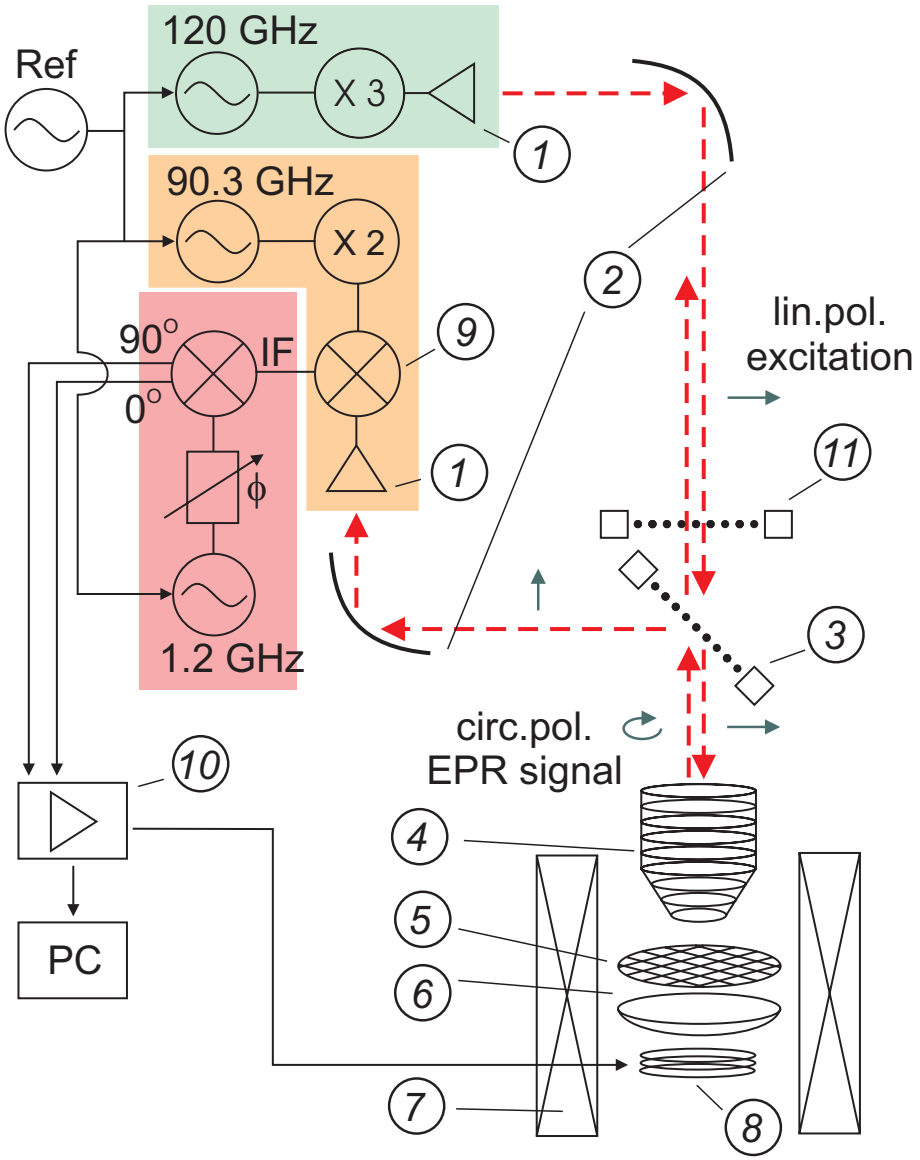

Figure 5.4: Experimental setup with corrugated horn antennas (1), off–axis elliptical mirrors (2), wire grid polarizer (3), tapered corrugated waveguide (4), coupling mesh (5), half–symmetric Fabry–Perot resonator (6) superconducting 14 T magnet (7), field modulation coils (8), subharmonic mixer detector (9), lock–in amplifier (10) and attenuator polarizer wire grid (11).

All focusing elements in our quasioptical transmission line therefore are metallic off–axis elliptical mirrors. Only inside the magnet bore the limited space requires the use of either lenses or a waveguide technique.

The main difficulty encountered when using conventional smooth–walled oversized waveguides is the excitation of higher order modes and the generation of standing waves at transition sections from and to fundamental mode waveguide.Originally introduced in the context of the transmission of high–power microwaves (J. L. Doane 1985), oversized corrugated waveguides provide the required low insertion losses and cross polarization artefacts (Smith et al. 1998, M. Thumm 1993).The incoming linearly polarized Gaussian beam couples with high efficiency to the hybrid HE_{11} mode of the corrugated waveguide which also has linear polarization and a Gaussian intensity profile. This implies a minimum electric mw field at the walls, whereby resistive losses and cross–polarization to the orthogonal mode are minimized.

This can be compared to the situation of smooth walled circular waveguides, where a linearly polarized Gaussian beam will couple to the TE_{11} and TM_{11} modes. Since those have differing phase velocities, a distorted beam profile may be the result.

To couple the microwave to the Fabry–Perot sample resonator, the output beam needs to be focussed down to a beam waist of 1.0 mm. This is achieved with a tapered section made of gold–plated copper at the end of the waveguide. The waveguide itself consists of 100 mm long electro formed sections with an overall length of 1080 mm. The diameter is 23 mm, being reduced by the taper over a length of 20 mm to 3 mm. The corrugation depth is 0.6 mm and the slot/metal pitch 0.25 mm. The material of the main section is German silver, which is preferred to copper since it has a lower heat conduction coefficient.

5.2.2 Induction Mode Operation

The linear polarization of the Gaussian beam is utilized in an induction mode detection scheme first described by (Teaney et al. 1961); later examples at high magnetic fields were introduced in transmission mode by (Prisner

et al. 1992) and reflection mode by (Smith et al. 1998).

The beam launched by the transmitter antenna has an initial beam waist ω_0 of 1.48 mm and is already linearly polarized. The first off–axis mirror focuses it onto the upper end of the corrugated waveguide to a beam waist of 7.24 mm.

On the way it passes through a wire grid polarizer that is oriented with an angle of 45° with respect to the optical axis. The free–standing wires (12 wires/mm, 25 μm diameter) will pass all radiation that is polarized perpendicular to the direction of the wires, since in this direction no currents can be induced, while radiation polarized along the wire direction is reflected. For initially uniformly polarized radiation the passed component with polarization along the wires is attenuated by approximately 20 dB compared to the unattenuated component. By mounting a second grid on a rotation stage in front of the first, one obtains a polarizer / analyzer setup that acts as a variable attenuator with a dynamic range of 20 dB. The rotation stage is slightly tilted with respect to the optical axis to avoid the buildup of standing waves in the system.

In the cylindrically symmetric Fabry–Perot resonator the excitation mw represents a composition of two circularly polarized modes with opposite polarization. Of those two modes only one can interact with the spin system and therefore becomes partially attenuated upon magnetic resonance. Recombined with the unattenuated component this yields elliptically polarized mw that is reflected into the waveguide.

Back at the wire grid polarizer only the component orthogonal to the excitation mw is reflected onto the receiver antenna, while the excitation power itself is passed to the transmitter tripler and attenuated there.

Essential in this context is the use of the cylindrically symmetric Fabry–Perot resonator as a bimodal cavity. Since all directions of polarization in the resonator are degenerate, both the excitation microwave and the EPR

induction component polarized orthogonally to it have to be supported by the structure. This also applies to the oversized waveguide transmission line. The use of a single mode cavity, despite many other advantages, is not feasible within an induction mode scheme.

The maximum obtainable isolation of excitation and detection arm is ultimately limited by the cross–polarized microwave component that is induced by the off–axis mirrors. This effect is partly corrected by the polarizer grid that is passed *after* the first mirror. Any other misalignment in the setup will also introduce cross–polarization. Overall this induction mode setup provides an attenuation of the excitation with respect to the EPR signal of 20 up to 30 dB.

The system as presented above can be compared to several alternative design approaches. While a transmission cavity can be constructed in an induction configuration, it is not possible to achieve critical coupling, i.e. destructive interference of the microwave component reflected at the resonator coupling interface with the component leaked from the resonator that is in antiphase. The general advantage of a transmission setup is that it does not require the use of a circulator or beam splitter type device to project the radiation coming from the cavity onto the detector.

In a reflection mode setup, it becomes necessary to separate the EPR signal from the reflected excitation microwave – in conventional EPR this is achieved with a circulator. In the present spectrometer this has been realized by utilizing the different polarization characteristics of of the signal and the excitation microwave. It can also be realized with the quasi–optical equivalent of a lambda–quarter plate / polarizer combination (Earle et al. 1996, Cardin et al. 1999) or with a Faraday rotator as decribed in the outlook in chapter 8. In this design, however, apart from the reduction in microwave background at the detector that can be achieved by properly matching the cavity, a further reduction is not possible. Imperfect critical

coupling and spurious reflections therefore have a much stronger influence on the spectrometer performance compared to the induction mode setup.

It should be stressed that one of the main principles underlying the current spectrometer design was to realize a setup with as few components as possible. This should ease proper alignment, minimize the generation of standing waves and allow to achieve low insertion losses. While due to the induction mode setup the overall insertion loss from transmitter to receiver horn cannot be directly measured, a conservative estimate based on the known performance of the separate components estimates it to 5 dB.

5.3 Resonator and Field Modulation

5.3.1 Resonator Design

Two different probeheads were used for the measurements. The first setup was shipped originally with the instrument and modified subsequently to include field modulation coils. (see figure 5.5).

Based on the experiences with this first setup, a second probehead was developed. On the EPR side, this probehead features better placed field modulation coils. The major new development, however, is the included RF circuit. With this extension, Electron Nuclear DOuble Resonance (ENDOR) experiments will become possible (see figure 5.6). It was developed by Yuri Grishin (Y. Grishin 1999) and will also be the topic of another "Doktor"–thesis (A. Schnegg 1999); the RF part will therefore not further be discussed here. The new probehead and the performance of its field modulation are discussed in subsection 5.3.2. Since the general design of the Fabry–Perot resonator and the tuning mechanism are identical for both designs, they will first be discussed together in the following.

The half–symmetric Fabry–Perot cavity is typically operated in the TEM_{006} mode (see figure 4.4), with $q = 6$ the number of half wavelengths in the cav-

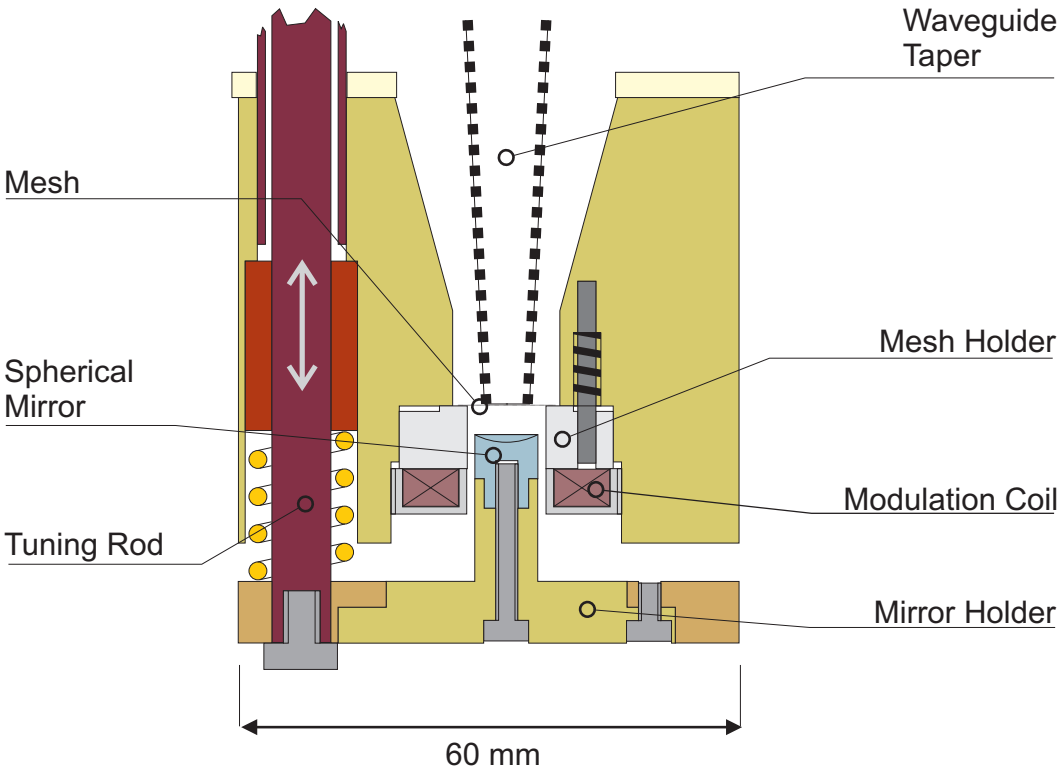

Figure 5.5: Original version of the probehead

ity. With a resonator distance $d = 2.58$ mm (equation 4.25) and curvature radius $R = 8.06$ mm one obtains a confocal distance $z_c = 3.76$ mm (equation 4.21). The resonator therefore is near–, but not semi–confocal, avoiding the degeneracy in the resonance frequency of the higher order modes.

Coupling to the tapered end of the corrugated waveguide is achieved through the flat mirror which actually is a highly reflective mesh (typically 30 wires / mm). The mesh consists of electroformed copper and is stretched onto an exchangeable mesh holder, where it is fixed with superglue onto a circular frame. Unless the measurements are to be performed at very low temperatures ($T < 100$ K), where overstretching of the meshes can become a problem, this approach has proven quite reliable.

The mesh holders were either made of aluminium or of Macor, a ceramic

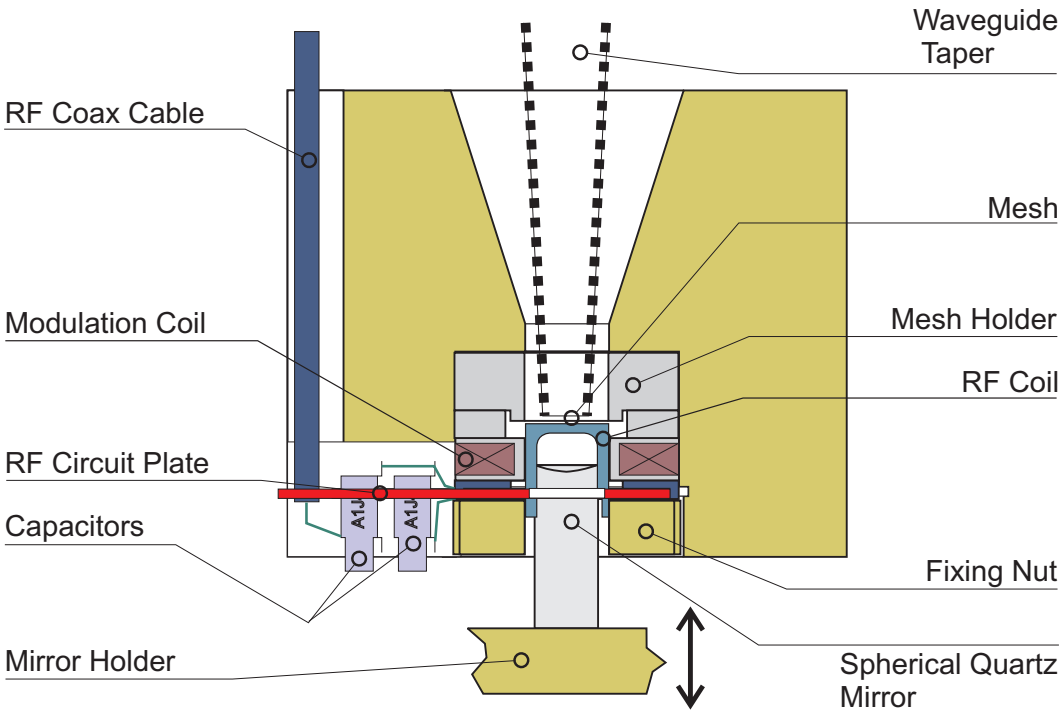

Figure 5.6: New version of the probehead with optimized positioning of field modulation coils and ENDOR RF circuit.

material that can be easily machined on a lathe. With the Macor holders, higher magnetic field modulation amplitudes could be achieved with equal modulation currents and were therefore preferred (see subsection 5.3.2).

Since the mesh holders are exchangeable, a mesh can be replaced by a mesh with a different reflectivity, thus allowing for variable coupling for different samples. Compared to a coupling mechanism that can be varied during the experiment, as it is commonplace in conventional EPR spectrometers, this is a rather imprecise procedure, of course. With some trial and error, however, it is possible to find meshes that allow for good coupling for the respective samples. Such a setup with a fixed mesh also provides much greater mechanical stability than one with a movable mesh; due to the higher sensitivity to vibrations at smaller wavelengths this was the deciding factor when opting for a fixed mesh.

Tuning is achieved by translating the spherical mirror via a micrometer screw and three brass rods (length is 1150 mm) from the top of the corrugated waveguide outside the magnet. The rods were guided by linear bearings at the top flange and by phosphor bronze sliding bushes in the probehead main body. Non–magnetic bronze springs at both ends serve as stabilizers. Since rods fabricated from stainless steel proved to exhibit enough residual magnetism to cause field inhomogeneities and therefore measurable line broadening, the rods were then constructed from copper and brass. To most closely match the thermal expansion coefficients of the phosphor bronze bushes to the rod material, the sections at the bottom were fabricated from copper, while the upper sections were made from brass to minimize thermal conduction. For temperatures below 100 K, a middle section of the rods can be replaced with aluminum or Macor rods to further minimize heat leaks. The use of copper as material for the lower sections of the tuning rods also was dictated by the need to match the expansion coefficient of the waveguide taper, which otherwise would touch or pierce the coupling mesh when cooled to low temperatures.

The actual performance of the resonator in terms of microwave field enhancement is best described by the quality factor Q or the resonator finesse F (Kogelnik & Li 1966).

With a conventional EPR spectrometer, Q can be measured directly by sweeping the microwave frequency f through its resonance value f_{res} and determining the full width at half maximum (FWHM) of the observed dip Δf_{FWHM}:

$$Q = \frac{f_{\mathrm{res}}}{\Delta f_{\mathrm{FWHM}}} \tag{5.2}$$

With our setup this is not feasible, since the source frequency cannot be swept.

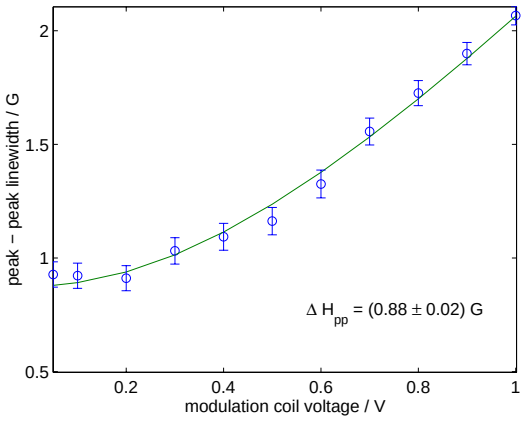

Figure 5.7: Calibration of modulation amplitude with $^{55}Mn^{2+}$ in MgO sample: first probe head design, small modulation amplitudes.

Instead, one can measure the resonator finesse F that is given by:

$$F = \frac{\Delta d_{\text{period}}}{\Delta d_{\text{FWHM}}} \tag{5.3}$$

with the FWHM of the resonator mode dip Δd_{FWHM} and the spacing between two consecutive dips Δd_{period}, both measured in terms of the relative mirror spacing.

Q can be obtained from F via the relation:

$$Q = (q-1)F \tag{5.4}$$

with the number of half wavelengths in the resonator q. For the purpose of assessing the performance of an EPR resonator, F is the more relevant quantity, since Q becomes arbitrarily large for high mode numbers without this leading to a higher field enhancement in a particular node.

A typical value for the finesse of the resonator with sample is $F = 160$, giving a result for the loaded Q–factor of this resonator of $Q = 800$.

5.3.2 Calibration of Field Modulation Amplitude

In the first setup, due to space restraints we have mounted the field modulation coils for Lock–In detection directly underneath the mesh holder and therefore also underneath instead of in the plane of the sample position. To

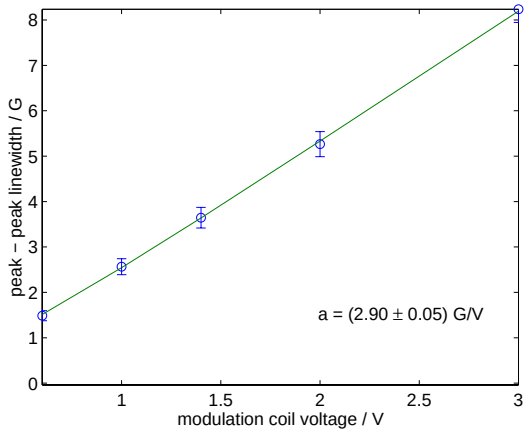

Figure 5.8: Calibration of modulation amplitude: like figure 5.7, large modulation amplitudes.

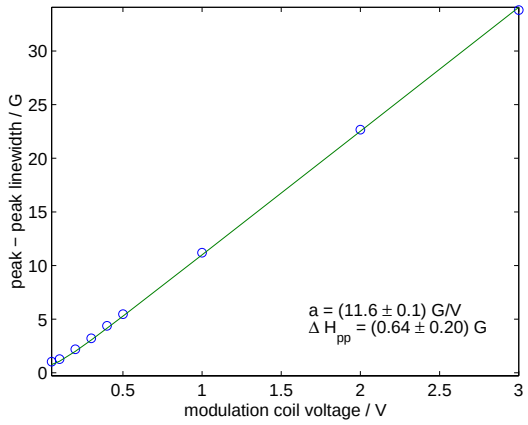

Figure 5.9: Calibration of modulation amplitude with Li/LiF sample: new probe head design.

minimize attenuation and microphonics effects both mesh– and modulation coil holder have been fabricated out of Macor. In that setup we can measure with modulation field strengths up to 1.5 mT.

The placement of the modulation coils in the new design is exactly around the sample location. This, as shown below, leads to higher modulation fields for equal currents in the modulation coils.

The modulation field amplitude can be calibrated by monitoring the observed linewidth of an intrinsically narrow EPR line with increasing modulation field amplitude. The observed peak to peak linewidth $\Delta H_{\mathrm{pp,obs}}$ in dependence of the applied modulation voltage amplitude V_{mod} can then be

fitted to the expression (Cardin et al. 1999, C. P. Poole 1967):

$$\Delta H_{\mathrm{pp,obs}} = \sqrt{\left(\frac{aV_{\mathrm{mod}}}{\Delta H_{\mathrm{pp}}}\right)^2 + 5 - 2\sqrt{4 + \left(\frac{aV_{\mathrm{mod}}}{\Delta H_{\mathrm{pp}}}\right)^2}} \tag{5.5}$$

This yields the intrinsic linewidth of the sample ΔH_{pp} and the coil calibration constant a.

The samples used were $^{55}Mn^{2+}$ in MgO polycrystalline powder and Li in LiF among others. Both have a narrow intrinsic linewidth $\Delta H_{\mathrm{pp,obs}}$ below 0.1 mT and therefore exhibit modulation broadening already for small modulation fields. They will be considered in more detail in chapter 7.

A comparison of the coil calibration constants a determined for the two different probehead setups (subsection 5.3.1) shows that the voltage needed to generate a specific modulation amplitude is smaller in the new setup by a factor of 4. For modulation coils with an equal number of windings and

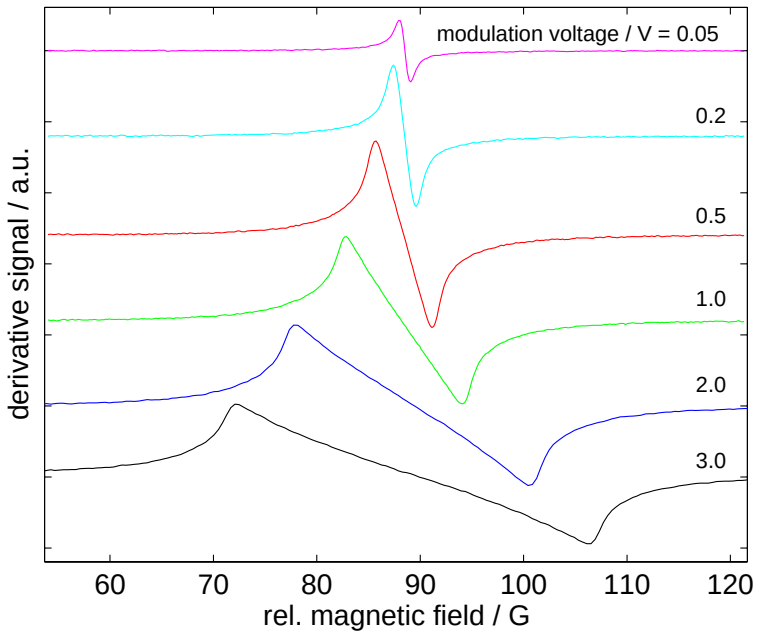

Figure 5.10: Li/LiF: Overmodulation of EPR line to allow for calibration of modulation amplitude. See figure 5.9 for fit to linewidths

identical wire, this also means that the current in the coil was reduced by the same amount. This greatly reduces the microphonics problems in the new setup and provides much higher mechanical stability of the cavity. Especially for the broad spectra of samples with an anisotropic g–tensor the larger modulation fields accessible with the new design will improve the achievable S/N by a considerable amount.

5.3.3 Resonator Tuning

The actual procedure of tuning the resonator is somewhat different to that of a standard EPR spectrometer. Since the source can not be swept over a wide enough frequency range, finding a resonant mode of the resonator requires tuning of the resonator mechanically while the microwave frequency remains fixed.

While the induction mode setup of the microwave bridge provides high isolation of the detector to the excitation microwave power as laid out above, the power coupled into the mode orthogonal to the excitation radiation is sufficient to monitor if power was actually coupled into the resonator. Upon finding a resonance dip, the only way to verify that it actually belongs to an EPR active fundamental TEM_{00n} mode, a real experiment has to be performed. When searching for resonances of an unknown species, the Mn^{2+} field calibration standard (section 7.1) therefore proves helpful also for deciding whether the mode is fundamental.

The microphonics problems described in subsection 5.3.2 can be alleviated by carefully tuning the resonator to resonance. Due to the modulation field being oriented parallel to the external magnetic field H_0, the vibrations causing the microphonics signal also modulate the resonator dimensions along the z–axis. This in turn causes a modulation of the position of the resonator dip on the frequency axis. The baseline offset due to the microphonics effect therefore has a zero crossing for the resonator tuned precisely to the reso-

nant mode. This can be used to minimize this offset, but also to tune more precisely to the resonance position in absence of a sweepable mw source.

5.4 Sample Handling

To minimize dielectric losses in the cavity due to the sample it has to be positioned at a point where the electric field has a node and the magnetic field has a maximum. In principle there are 3 choices – placing the sample on the flat coupling mesh, in a flat sample cell in a node close to the mesh or directly on the mirror surface.

In the current setup, we chose to place the sample directly on the mirror. This has the disadvantage of a lower H_1 field at the sample position (80% of the value at the beam waist directly on the coupling mesh – see figure 5.11). Also, the curvature of the surface causes some problems when trying to apply flat films tightly to the surface. To obtain a usable mode, the sample thickness has to stay well below 0.1 mm.

If the sample is placed directly on the mesh, the handling is much more problematic yet since the mesh is extremely delicate and therefore easily

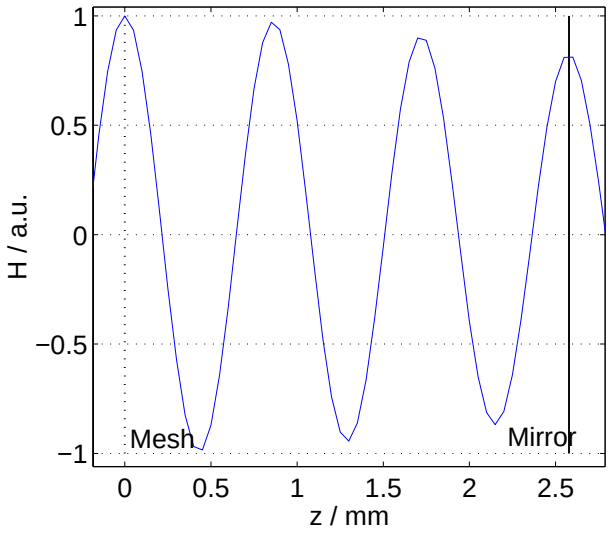

Figure 5.11: Magnetic field amplitude at the FP resonator symmetry axis for the TEM_{006} mode. The coupling mesh sits at $z = 0$ mm, the curved mirror at $Z = 2.58$ mm.

destroyed. Also, the coupling of the waveguide to the cavity can be strongly influenced by a sample placed directly on the mesh. This has been observed for the case of coupling irises (Barnes & Freed 1997).

The advantage to placing the sample in a flat cavity in an E–field node in free space is that with the sample placed directly on the mirror, no independent adjustment of the sample position is necessary when tuning the cavity.

The current method clearly is a compromise where we opted for greater reliability and mechanical stability instead of maximum performance.

Placing samples on the mirror surface was done in different ways depending on the type of sample:

- Polycrystalline samples were usually dissolved in a solvent, applied to the mirror surface and the solvent let evaporate. The recrystallized powder then stuck to the surface and no further treatment was necessary.

- Small single crystals could be fixed to the surface with minuscule amounts of vacuum grease.

- The samples used for sensitivity measurements and the Mn^{2+} standard sample were prepared dissolved in a polystyrene film. This gives the possibility to apply known amounts of spins by simply weighing the film when the concentration of the solute is known. Also, the film protected the sample from water and other solvents if more than one sample was placed on the mirror. This was very important for the Mn^{2+}/MgO powder that degrades immediately when coming in contact with water.

  To attach a polystyrene film flat to the curved mirror surface, a small amount of toluene was applied to a small piece of film on the mirror so the film became soft and followed the curvature. After drying, a second

sample could be placed next to the film, since the sample in the film was practically sealed.

- Samples in water or water / glycerol mixtures (e.g. proteins) were applied to the mirror by pressing a thin piece of Mylar–foil directly on a small drop of the sample (substance name: Polyethyleneterephtalat by Goodfellow Ltd, thickness 0.05 mm). The Mylar foil had been brought into a curved shape by heating it up in a template mirror with identical dimensions as the real one.

  While this approach has only been used for measurements with frozen solutions (around 200 K), it should easily work at room temperature as well.

- A second way of applying highly viscous liquid samples to the mirror consisted in lowering the surface tension of the mirror surface with a minuscule amount of detergent. We chose n–octyl–β–D–glucopyranoside (SigmaUltra O 9882), a non–ionic detergent that is frequently used in the preparation of protein–crystals. Care was taken to use a detergent concentration below the critical denaturing concentration (Gould et al. 1981).

- Water–containing samples were also applied to the curved mirror surface by absorbing them into a thin cellulose tissue. This approach will not work with samples sensitive to oxidation, since the surface increases due to the fine structure of the tissue.

5.5 Spectrometer Sensitivity

The absolute sensitivity of different EPR spectrometers can be compared by quoting the minimum number of detectable spins $N_{\min}$ per G (= 0.1 mT)

linewidth detected with a detection bandwidth of 1 Hz. $N_{\min}$ is given as

$$N_{\min} = \frac{N}{S_N n_L \Delta B_{\mathrm{pp}} \left(B_{\mathrm{Mod,\ opt}}/B_{\mathrm{Mod,\ real}}\right)} \tag{5.6}$$

where S_N is the signal to noise ratio and ΔB_{pp} is the peak to peak linewidth of the derivative EPR line of a single spectrum acquisition. n_L is a correction factor to account for cases where a spectrum consists of more than one line and only one of these is considered in the sensitivity measurements, such as is the case for our Mn field calibration standard (section 7.1). The factor $B_{\mathrm{Mod,\ opt}}/B_{\mathrm{Mod,\ real}}$ is a correction factor for cases where the field modulation amplitude employed in the measurement $B_{\mathrm{Mod,\ real}}$ is less than the optimum modulation amplitude $B_{\mathrm{Mod,\ opt}}$ (usually equivalent to the peak to peak linewidth ΔB_{pp}).

To obtain a sample with a known number of spins, the substances were dissolved in a highly viscous solution of polystyrene polymer in toluene. This solution was then homogenized by stirring for an extended time (important for the Mn sample which actually is a dispersion). The solution was then spread onto a glass plate and the solvent let evaporate to yield a thin polystyrene film. Larger patches of this film were weighed on a high precision scale. The absolute number of spins in the final sample was then determined by the ratio of sizes between weighed film and final sample. Typically, in all measurements the number of spins in the resonator was 10^{14}. The minimum number of detectable spins $N_{\min}$ determined by this procedure is as high as $5 \cdot 10^9$ Spins/G at a lock–in detection bandwidth of 1 Hz.

5.6 Numerical Phase Correction

In an EPR experiment, one usually wants to detect the microwave absorption signal. It can be described quantitatively by the imaginary part χ'' of the susceptibility $\chi = \chi' - i\chi''$ which gives the contribution of the sample magnetization M in the direction perpendicular to the vector of the microwave

field B_1 ($\chi'' = M_\perp / B_1$) (Schneider & Plato 1971). The real part $\chi' = M_\parallel / B_1$ describes the dispersion signal. If the EPR transition is not saturated, the two signals are related via the Kramers–Kronig relations:

$$\begin{aligned} \chi'(\omega) &= \frac{1}{\pi} \int_{-\infty}^{+\infty} \frac{\chi''(\omega')}{\omega' - \omega} \, d\omega' \\ \chi''(\omega) &= -\frac{1}{\pi} \int_{-\infty}^{+\infty} \frac{\chi'(\omega')}{\omega' - \omega} \, d\omega' \end{aligned} \tag{5.7}$$

χ' and χ'' are said to be Hilbert transforms of each other (Killingbeck & Cole 1971, Mathews & Walker 1973).

In the present experimental setup the detected signal can display an admixture of dispersion. Since the spectrometer uses a phase–locked source, we can not use automatic frequency control (AFC) to keep the measurement frequency tuned to the cavity resonance. If the resonator is not precisely tuned to the measurement frequency, or if the mirror positions shift slightly due to vibrations or temperature variations, the dispersion signal will be detected in addition to the absorptive component. Another reason for the detection of a dispersive component can be a standing wave background signal at the detector with a phase shifted relative to the actual EPR signal. Also, the shift in effective cavity frequency at EPR resonance for very strong signals can introduce a significant dispersion signal.

The relationship between absorption and dispersion expressed in equation 5.7 can then be used to numerically correct phase errors (Earle et al. 1993). Via a numerical Hilbert transform, the 90° out–of–phase ("quadrature") component of the detected signal is computed and a linear combination of the resulting signals is added to obtain the absorption signal. A crucial requirement for this technique is a constant phase offset of the entire spectrum. Varying phase variations due to a resonator drift during the acquisition of a spectrum or a phase shift due to a strong EPR signal can therefore not be corrected by this method. All spectra with a constant phase offset were corrected by adjusting the phase manually and making sure that the integrated

signal correctly returned to a zero baseline.

5.7 Magnet and Cryostat

The superconducting magnet is a Teslatron H system (Oxford Instruments 1997). It can sustain a magnetic field of up to $B_0 = 14$ T. All experiments were run with a central magnetic field $B_0 = 12.846$ T, the resonance field for the free electron g–value and a microwave frequency of 360 GHz. The lowest accessible g–value with a 14 T central field is $g = 1.84$.

Integrated into the main coil assembly is a superconducting sweep coil with a sweep range of ±100 mT. This way the magnet can be swept with a sweep rate of up to 70 mT/min while the main coil remains in persistent mode.

The homogeneity of the magnet is specified to 3 ppm in a 10 mm sphere. This was verified with an NMR Gaussmeter with a Deuterium probe that was moved along the symmetry axis of the magnet (figure 5.12).

The linearity of the field sweep has also been tested with an NMR gaussmeter for a full sweep upon installation. As can be seen in figure 5.13, the sweep is not linear and after a half cycle, a remanent field of 4 mT can be observed. After a full cycle the field offset was 0.05 mT. This necessitates the use of a standard sample for magnetic field calibration (section 7.1).

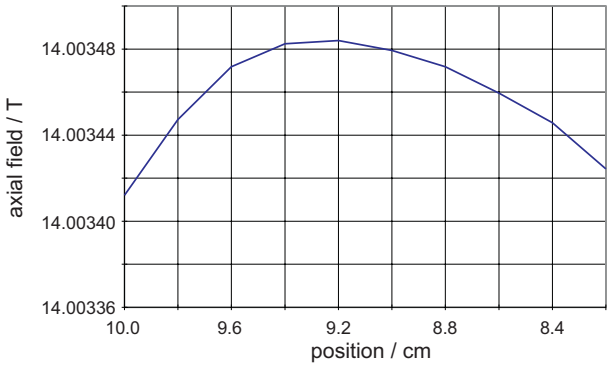

Figure 5.12: Oxford Instruments Teslatron H magnet: plot of axial field variation around maximum field at 14 T.

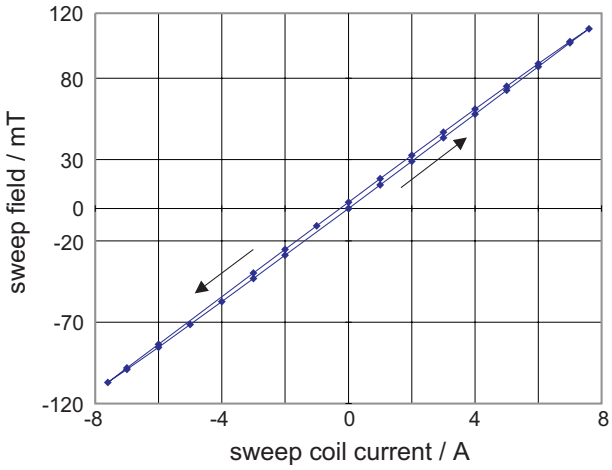

Figure 5.13: Oxford Instruments Teslatron H magnet: plot of sweep field vs. sweep coil current around center field at 14 T. The direction of the sweep is indicated with arrows. The remanent field after a half cycle is 4 mT, after a full cycle it is 0.05 mT.

The warm bore of the magnet has a diameter of 88 mm. We could therefore employ a cryostat with a rather large probehead space diameter of 62 mm.

The cryostat is a Helium–cooled static flow cryostat (Oxford Instruments CF1200) which offers a temperature range of 3.8 K to 300 K. In a static flow design, the probehead is not cooled directly by the He vapor. Instead, the Probehead space is closed off and filled with a buffer gas (we used Argon) which in turn is cooled by a Copper heat exchanger shield that is in direct contact with the Helium. This setup avoids stability problems that often arise in direct flow designs.

5.8 Experiment control software

5.8.1 The LabVIEW programming environment

The spectrometer control and data acquisition during an experiment is handled via a personal computer. The software performing these tasks will be described in the following section.

The programming environment used for the task is the LabVIEW package for Microsoft Windows 9x (National Instruments 1998). The actual programming language contained in the package is the graphical programming language "G".

Its most distinctive difference to the commonly used programming languages "C" or "C++" is the graphical structure of the program code. A program in G consists not of successive lines of programming code that are executed one after another during runtime ("control flow execution"). Instead, the order of execution of commands is governed by the availability of data or information at the input of subfunctions in the program code ("data flow execution"). All operators (such as an addition or a comparison) and subfunctions (such as an instrument readout) in a program are only related via the variables that are passed between them and are executed by the engine immediately once all data inputs are present.

This approach is particularly suited for a programming task such as experiment control, where, due to the constant interaction with the spectrometer operator, a strictly linear program execution is not a given. The data control structure becomes obvious in the graphical representation of the program code. It mainly consists of icons that represent functions and operators. These in turn are connected with lines that each represent a variable being passed between them.

The most important reason to choose LabVIEW as the programming language, however, was its integrated graphical user interface. While providing

a visual display of the acquired data on the computer screen and generating a graphical interface for user input can be a very tedious task with a programming language like C, in LabVIEW the necessary routines are readily provided with the package.

Last but not least, LabVIEW is strictly object oriented, which should make it very easy for different authors to add new modules to the program later when the need arises.

5.8.2 The EPR program modules

The main program for running the spectrometer is called "*submm*". Its EPR measurement part consists of two different components: a free–sweep monitor module and a dedicated data acquisition module.

The monitor module is used during the process of searching for a signal and optimizing field modulation parameters. The user has a simple "up", "down" and "stop" control of the magnetic field sweep. The screen is continually updated with the signal input from the lock–in amplifier vs. the sweep coil current. Other parameters that can be modified in this mode are field sweep rate and several lock–in amplifier parameters such as the data acquisition rate or the time constant.

Once the resonator has been successfully coupled and the signal position has been found, the user can switch to the second, the data acquisition unit. Here the magnet is swept with a fixed rate between two points on the magnetic field axis. This part of the program will run continually until the operator decides that a sufficient amount of data averaging has been achieved and interrupts the program. The data can then be saved.

5.8.3 Data structure

The data acquisition generally always saves every single sweep, not the averaged data. This file is a pure text file in spreadsheet form that can be directly imported into the Matlab numerical mathematics environment (The Mathworks, Inc. 1999) that is used for further data processing and plotting. The actual averaging of the data is then done in a Matlab routine called "*mmdat*". It allows the user to separately view the single sweeps belonging to a data set and compare them to the average of an arbitrary selection of single sweeps. The data can thus be checked for artefacts due to temporary instabilities of the spectrometer or baseline drifts. All sets that are free of artefacts can then be averaged and saved. In addition to this, the *mmdat* routine can be used as a quick browser for experimental spectra.

The header of each data file contains the values of all variables set by the program at the start of each acquisition. The *submm* acquisition program is able to re–import such a data file. All measurement parameters are then directly set to the instruments. This greatly facilitates to perform a second set of experiments under identical conditions as a previous one.

Apart from the acquisition data files, the *submm* program allows the user to save setup parameter files for each instrument. At the start of an experiment these parameter files can be read in to ensure that all instruments are in a standard condition.

5.8.4 Experiment timing

A critical point for hardware handling programs in multitasking operating systems such as Microsoft Windows, Linux or Unix is the timing. In the case of the *submm* program it was necessary to ensure that the current of the magnetic field sweep coils followed a linear ramp and that data points were sampled at constant intervals.

The choice usually has to be made to either use the PC as a master clock or to slave all other instruments to a master clock provided by one instrument. Since Windows, as mentioned above, has no true real–time capabilities, the first approach would imply the need for additional timing hardware to be included in the computer.

This turned out not to be necessary since both the lock–in amplifier and the sweep coil power supply (Oxford IPS–20) provide internal timing clocks. The power supply can be set to fixed current sweep rates k_C between $k_C = 0.01$ A/min and $k_C = 200$ A/min with very high time and current resolution (0.1 mA).

The lock–in amplifier has a large internal buffer for over 16000 data points, that can be stored with a variable data acquisition rate. The data can then be transferred continually to the computer during acquisition, without actually interfering with the timing of the experiment. Together this allows the *submm* program to hand over the timing–critical operations to the more precise modules of the power supply and the lock–in amplifier. It also enables the operator to run additional software parallel to the experiment, such as the Matlab environment for data processing or data transfer to networked computers.

5.8.5 Interfacing

All hardware components provided control interfaces that support the IEEE 488.2 protocol (General Purpose Interface Bus GPIB). In the case of the Oxford Instruments power supply, all instruments share one GPIB interface on the Oxford temperature controller that functions as a master gateway to the so–called Oxford ISO Bus. This is a modified RS 232 serial port that allows communication to up to 8 additional Oxford instruments such as the liquid He level meter, main coil power supply, temperature controller, etc.

There are two more instruments that can be interfaced to the measure-

ment program: a digital oscilloscope Tektronix TDS 744A and a radio frequency generator HP 8648B.

The TDS routine establishes the GPIB interfacing to the component and mainly serves to read out data to the computer. Apart from recording test results monitored directly with the oscilloscope, this is a possibility to record data sets from the HP spectrum analyzer which only has an analog output.

The HP RF synthesizer module also establishes the interfacing and records and sets the instrument state. This part of the program will be used with the expansion of the spectrometer to ENDOR experiments.